Monatshefte für Chemie 131, 251–265 (2000)

Monatshefte für Chemie
Chemical Monthly

Carbene Complexes of Pnictogen Pentafluorides and Boron Trifluoride

Anthony J. Arduengo III,[1,*] **Fredric Davidson,**[2] **Roland Krafczyk,**[1] **William J. Marshall,**[2] and **Reinhard Schmutzler**[1]

[1] Institut für Anorganische und Analytische Chemie der Technischen Universität Braunschweig, D-38023 Braunschweig, Germany
[2] DuPont Science and Engineering Laboratory, Experimental Station Wilmington, Delaware 19880-0328, USA

Summary. Synthesis, characterization, and solid state X-ray crystallographic structures for 12-*Pn*-6 complexes derived from carbene 4,5-dichloro-1,3-dimesitylimidazol-2-ylidene and phosphorus, arsenic, or antimony pentafluoride are reported. The adducts show octahedral geometries at the pnictogen centers with C-*Pn* bond distances of 189.8 (P), 199.9 (As), and 217.5 (Sb) pm. The structures are those of internal zwitterions with imidazolium ion character in the heterocyclic ring and a pentafluoropnictanide anion bonded to C^2. Adducts of BF_3 with 1,3-dimesitylimidazol-2-ylidene and 4,5-dichloro-1,3-dimesitylimidazol-2-ylidene are also reported for comparison. Although the reactivity of chlorinated and non-chlorinated carbenes varies considerably, the spectroscopic and structural properties of analogous adducts are remarkably similar.

Keywords. Carbene; Pnictogen(V) fluorides; Boron(III) fluoride; Zwitterions; Imidazol-2-ylidene.

Introduction

The reaction of nucleophilic carbenes with various *Lewis* acids provides access to a wide variety of carbene adducts [1–3]. Even weak electrophiles like alkali metal cations [4–6], IC_6F_5 [7], $Sb(CF_3)_3$ [8], and $Cd(CH_3)_2$ [9] readily form adducts with highly nucleophilic imidazol-2-ylidenes. However, with very aggressive electrophiles such as the pnictogen pentafluorides (PnF_5; $Pn = P$, As, Sb), simple adduct formation with imidazol-2-ylidenes is difficult to control because of the extreme reactivity of these two components. It is also important to choose a solvent that is simultaneously compatible with a very strong nucleophile and a very strong electrophile and thus offers favourable solubility properties for the reaction. We now report that the chlorinated imidazol-2-ylidenes are excellent reaction partners for highly aggressive electrophiles and 1,3-*bis*(trifluoromethyl)benzene is an suitable reaction medium for highly reactive electrophiles such as AsF_5 and SbF_5.

---

[*] Corresponding author

Results and Discussion

As reported for 1,3,4,5-tetraalkylimidazol-2-ylidenes [10], carbene **1** [11] reacts with boron trifluoride etherate in *THF* solution to give the simple 1:1 adduct $\mathbf{1}\cdot BF_3$ in 82% yield (Eq. (1)). Tetrahydrofuran is an acceptable solvent for this reaction as long as $BF_3\cdot OEt_2$ does not contact *THF* in the absence of the carbene; otherwise, the BF_3 catalyzed polymerization of *THF* begins to interfere with adduct formation.

Under all circumstances PF_5 is incompatible with *THF*. Reaction of carbene **1** with PF_5 in toluene proceeds according to Eq. (2) to produce the 12-P-6[1] adduct $\mathbf{1}\cdot PF_5$ as minor product (~25% of the reaction mixture with 1,3-dimesitylimidazolium hexafluorophosphate, $\mathbf{1}\cdot HPF_6$). In contrast, however, when 4,5-dichloro-1,3-dimesitylimidazol-2-ylidene (**2**, [12]) was allowed to react with PF_5 in toluene, the adduct $\mathbf{2}\cdot PF_5$ was isolated in about 60% yield (Eq. (3)).

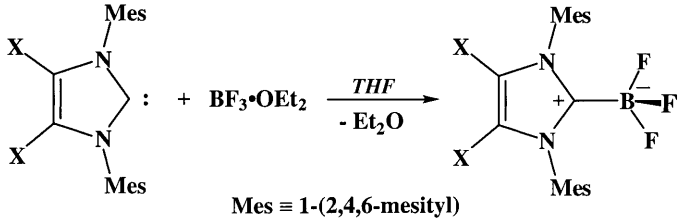

(1)

1 ($X = H$) $\mathbf{1}\cdot BF_3$ ($X = H$)
2 ($X = Cl$) $\mathbf{2}\cdot BF_3$ ($X = Cl$)

The improvement in adduct formation by the use of **2** is likely the result of the moderation of the carbene's nucleophilic reactivity by the inductive effect of the two chlorine substituents. Additionally, the acidic protons on $C^{4,5}$ of the product imidazolium ions are absent so that they cannot be lost to bases in the reaction

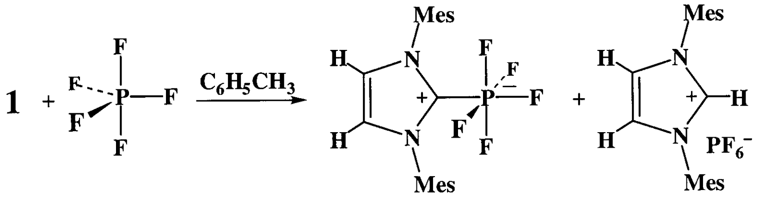

(2)

$\mathbf{1}\cdot PF_5$ $\mathbf{1}\cdot HPF_6$

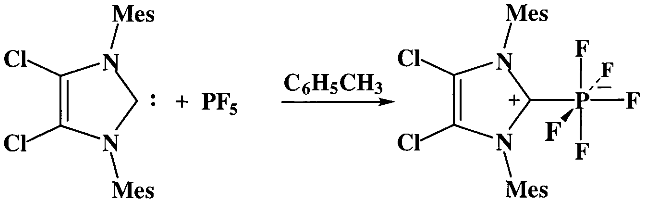

(3)

2 $\mathbf{2}\cdot PF_5$

---

[1] The *N-X-L* nomenclature system has been previously described (*N* valence electrons about a central atom *X* with *L* ligands); see: Perkins CW, Martin JC, Arduengo AJ, III, Lau W, Algeria A, Kochi JK (1980) J Am Chem Soc **102**: 7753

medium. Unlike the PF_5 reaction with carbene **1**, a C^2-protonated imidazolium ion was not obtained when **2** was the reaction partner for PF_5.

Arsenic and antimony pentafluorides are not compatible with toluene as a reaction medium. Various fluorochlorocarbons also proved to be unsatisfactory solvents for the reactions of AsF_5 or SbF_5 with carbene **2**. An excellent solvent for the reaction of the heavier pnictogen pentafluorides with **2** is 1,3-*bis*(trifluoromethyl)benzene from which the carbene-pnictogen pentafluoride adducts $2 \cdot AsF_5$ and $2 \cdot SBF_5$ could be isolated in 65% and 77% yields, respectively (Eq. (4)).

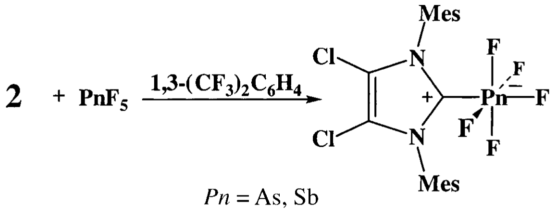

2·PnF5

(4)

The adduct $\mathbf{1} \cdot PF_5$ proved to be not only difficult to synthesize but also to purify. Attempts to recrystallize $\mathbf{1} \cdot PF_5$ from *THF* led to decomposition accompanied by the formation of $\mathbf{1} \cdot HPF_6$ and additional unidentified byproducts. In contrast, all adducts derived from the chlorinated carbene **2** can easily be recrystallized from *THF* or *THF*/toluene mixtures. Adducts from the less electrophilic boron trifluoride are also easily handled and recrystallized regardless of the carbene (**1** or **2**) used as the donor. The chlorinated carbene adduct $\mathbf{2} \cdot BF_3$ can even be recrystallized from hot acetonitrile without decomposition.

Compared to many of the previously isolated adducts of imidazol-2-ylidenes with weak electrophiles, the adducts from BF_3 and PnF$_5$ do not appear to undergo a facile dissociation to their starting materials (*vide infra*). The ^{13}C chemical shifts of the former carbene centers suggest a strong boron or pnictogen bond to the C^2 center of the imidazole fragment. These ^{13}C resonances are not always easily observed in the PnF$_5$ or BF_3 adducts because of their multiplicity and/or quadrupolar broadening. In all cases for which these data are available, the chemical shifts fall within a narrow range ($\delta = 158$–163 ppm) approximately 60 ppm upfield of the resonances of the corresponding carbene. This chemical shift range is close to the previously reported resonances for the C^2 centers in adducts of carbene **1** and phenyltetrafluorophosphorane ($\mathbf{1} \cdot PF_4Ph$) [13] or methyltetrafluorophosphorane ($\mathbf{1} \cdot PF_4CH_3$) [14] ($\delta = 164.7$ and 163.9 ppm, respectively).

For the BF_3 adducts, a single fluorine resonance is observed at $\delta = -142.4$ ppm ($^{1}J_{^{11}\mathrm{B}^{19}\mathrm{F}} = 34.6$ Hz) or $\delta = -142.6$ ppm $^{1}J_{^{11}\mathrm{B}^{19}\mathrm{F}} = 32.4$ Hz) in $\mathbf{1} \cdot BF_3$ and $\mathbf{2} \cdot BF_3$, respectively. The corresponding ^{11}B resonances occur at $\delta = -1.36$ and $\delta = -1.65$ ppm. The phosphorus centers in $\mathbf{1} \cdot PF_5$ and $\mathbf{2} \cdot PF_5$ show ^{13}P resonances of $\delta = -151.3$ and -151.8 ppm that are also quite similar to one another. As observed for the corresponding pair of BF_3 adducts, the heteroatom resonance (^{11}B or ^{31}P) for the adduct derived from the chlorinated carbene (**2**) occurs at slightly higher field than that for the adduct derived from carbene **1**. The difference in these shifts is, however, very small so that it is not possible to make generalizations about the relative electron donating abilities of these two carbenes based upon these data.

Table 1. Selected bond lengths (pm) and angles (°) in carbene adducts of BF_3 and PnF_5

	$\mathbf{1}\cdot BF_3$	$\mathbf{2}\cdot BF_3$	$\mathbf{2}\cdot PF_5$	$\mathbf{2}\cdot AsF_5$	$\mathbf{2}\cdot SbF_5$
$r(C^2\text{-}E)$	163.5(5)	166.9(6)	189.8(3), 189.8(3)	199.1(6), 200.6(5)	217.5(5)
$r(E\text{-}F)$	132.3 (aver)	136.5 (aver)	160.0 (*eq*) 159.6 (*ax*) 158.9 (*eq*), 159.2 (*ax*)	172.6 (*eq*) 170.9 (*ax*) 171.0 (*eq*), 171.6 (*ax*)	186.6 (*eq*), 186.3 (*ax*)
$r(C^2\text{-}N^{1(3)})$	135.0(5), 135.3(5)	136.3(8), 134.1(8)	136.2(4), 135.8(4) 135.9(4), 137.7(4)	136.6(7), 135.7(7) 135.4(7), 135.0(7)	135.6(6), 137.3(6)
$r(N^{1(3)}\text{-}C^{5(4)})$	137.6(5), 138.8(5)	137.2(9), 137.7(9)	140.0(4), 139.9(4) 139.2(4), 138.0(4)	138.1(7), 137.4(7) 139.5(7), 138.1(7)	138.0(6), 138.9(6)
$r(C^4\text{-}C^5)$	133.0(5)	132.8(10)	134.4(5), 134.3(5)	134.1(7), 135.1(7)	132.3(7)
$\theta(N^{1(13)}\text{-}C^2\text{-}E)$	128.0(4), 127.0(4)	126.4(4), 127.0(4)	125.7(2), 127.4(2) 127.1(2), 127.4(2)	126.4(4), 127.5(4) 126.0(4), 126.8(4)	127.6(3), 127.2(3)
$\theta(F\text{-}E\text{-}F)$	108.5 (aver)	110.2 (aver)	90.4 (*cis*), 178.2 (*trans*) 90.5(*cis*), 177.9 (*trans*)	90.1 (*cis*), 179.1 (*trans*) 90.1 (*cis*), 179.1 (*trans*)	89.8 (*cis*), 179.1 (*trans*)
$\theta(C^2\text{-}E\text{-}F)$	110.4 (aver)	108.7 (aver)	89.2 (*eq*) 178.8 (*ax*) 89.0 (*eq*), 179.3 (*ax*)	89.8 (*eq*) 179.2 (*ax*) 89.7 (*eq*), 178.7 (*ax*)	90.5 (*eq*) 179.0 (*ax*)
$\theta(N^1\text{-}C^2\text{-}N^3)$	105.0(3)	103.8(5)	106.9(3), 105.1(3)	106.0(4), 106.7(4)	105.2(4)
$\theta(C^2\text{-}N^{1(3)}\text{-}C^{5(4)})$	110.6(3), 110.1(3)	110.8(6), 111.5(6)	109.0(2), 109.1(3) 110.4(4), 109.6(3)	109.4(4), 109.4(4) 109.5(4), 109.4(4)	109.6(4), 109.6(4)
$\theta(N^{1(3)}\text{-}C^{5(4)}\text{-}C^{4(5)})$	107.3(4), 107.0(4)	107.1(7), 106.7(7)	107.4(3), 107.6(3) 106.6(3), 108.1(3)	107.1(4), 108.1(4) 106.4(4), 107.9(4)	108.6(4), 107.0(4)
$\phi(\text{imid}^{(C2)}\text{-}E)$	0.91	1.29	1.48, 5.28	2.21, 5.82	1.17
$r(\text{imid}^{(\text{plane})}\text{-}E)$	3.3	2.1	5.8, 20.5	7.0, 23.0	4.9

The *Pn*F_5 adducts show two magnetic environments for the fluorine centers. These two fluorine signals occur in a 1:4 ratio and correspond to the axial (opposite of the carbene) and equatorial (adjacent to the carbene) fluorine sites. The geminal ^{19}F-^{19}F couplings in the two phosphorus adducts (**1** · PF_5 and **2** · PF_5) amount to 54.4 and 55.2 Hz, respectively. In the case of **2** · AsF_5 $^2J_{^{19}F^{19}F}$ (111.7 Hz) is considerably larger than in the phosphorus analogs. The fluorine resonances for the antimony adduct (**2** · SbF_5) were too broad to allow the observation of F-F coupling. The resonance of C^2 in **2** · SbF_5 was also not detected. These broadening effects on C^2 and F in **2** · SbF_5 are most likely the result of influences from the adjacent quadrupolar antimony nuclei.

Structural investigations

There are no X-ray structural data of BF_3 adducts of imidazol-2-ylidenes available in the literature. Within the context of comparing adducts derived from imidazol-2-ylidenes with those from their more stable chlorinated analogs, we decided to examine the boron adducts reported herein. Crystals of **1** · BF_3 and **2** · BF_3 were grown from hot acetonitrile and toluene, respectively. Their solid state structures are depicted by KANVAS[2] drawings in Figs. 1 and 2. Selected bond lengths and angles are provided in Table 1.

The imidazole ring in **1** · BF_3 is nearly planar with no atom deviating more than 0.5 pm from the mean plane. The boron atom lies 3.3 pm out of the plane of the imidazole ring, and the boron center is displaced only 0.9° from the idealized imidazole 2-fold axis. The nitrogen centers are essentially planar with N^1 and N^3 lying only 1.2 pm out of the planes of their three attached atoms. The BF_3 group is rotationally disordered, and the positions of the fluorine atoms can be modelled by a set of two rotamers orientated approximately 60° from one another. The N–C–N

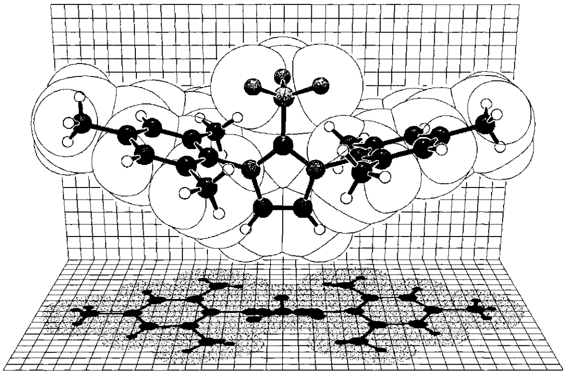

Fig. 1. KANVAS drawing of **1** · BF_3 (only a single orientation of the disordered BF_3 group is illustrated)

---

[2] The KANVAS program is based on the program SCHAKAL by *E. Keller* (Kristallographisches Institut der Universität Freiburg, Germany) which was modified by *A. J. Arduengo III* to produce the back and shadowed planes. The planes bear a 50 pm grid, and the light source is at infinity so that the shadow size is meaningful.

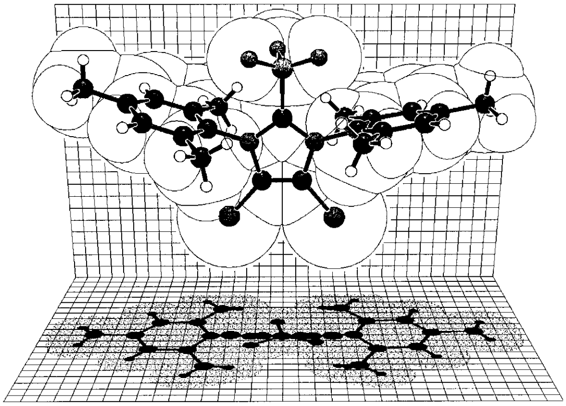

Fig. 2. KANVAS drawing of $\mathbf{2} \cdot BF_3$

angle at the former carbene center of $\mathbf{1} \cdot BF_3$ is 105.0(3)°. The C^2–B bond distance in $\mathbf{1} \cdot BF_3$ is 163.5 (5) pm. The overall geometry observed for $\mathbf{1} \cdot BF_3$ is similar to that of a borane (BH_3) adduct of 1,3-diethyl-4,5-dimethylimidazol-2-ylidene except for a shorter C^2–B distance (160.3(3) pm) in the borane adduct.

For $\mathbf{2} \cdot BF_3$, the imidazole ring is also nearly planar, with no atom deviating more than 0.3 pm from the average plane. The boron atom lies 2.1 pm out of the plane of the average imidazole ring and is displaced 1.3° from the idealized imidazole 2-fold axis. The nitrogen centers are essentially planar, with N^1 and N^3 rising only 0.8 and 3.5 pm out of the planes of the three attached atoms. The boron is at the center of a fairly regular tetrahedron with an average C^2–B–F angle (108.7°) that is only slightly smaller than the average F–B–F angle (110.2°). The N–C–N angle at the former carbene center (106.6(3)°) is slightly larger than observed in $\mathbf{1} \cdot BF_3$ (105.0(3)°), and the C^2–B bond distance of 166.9(6) pm in $\mathbf{2} \cdot BF_3$ is significantly longer than in $\mathbf{1} \cdot BF_3$ (163.5(5) pm. The longer C^2–B distance in $\mathbf{2} \cdot BF_3$ may be an indication of a weaker carbon–boron bond than in $\mathbf{1} \cdot BF_3$ due to the electron withdrawing chlorine atoms at C^4 and C^5. There is essentially no difference in the C^4–C^4 bond distances between $\mathbf{1} \cdot BF_3$ and $\mathbf{2} \cdot BF_3$. This similarity suggests that there is no great steric or electronic replusion between the adjacent chlorine centers in $\mathbf{2} \cdot BF_3$.

As reported above, $\mathbf{1} \cdot PF_5$ was too liable to allow easy production of X-ray quality crystals. Repeated attempts to recrystallize $\mathbf{1} \cdot PF_5$ led only to the isolation of $\mathbf{1} \cdot HPF_6$. Adventitious water does not appear to be the problem in handling $\mathbf{1} \cdot PF_5$. It is likely, however, that a PF_5 moiety on C^2 sufficiently acidifies the $H^{4,5}$ protons so that other decomposition pathways become important.

The PnF$_5$ adducts derived from carbene **2** all can easily be handled and were conveniently recrystallized from *THF* or toluene/*THF* mixtures to produce crystals suitable for X-ray structure determination. The phosphorus and arsenic adducts are isomorphic and crystallize in the monoclinic space group *C*c with two independent molecules of the adduct in the unit cell. In the subsequent discussion the structural data for the second independent molecule are given in square brackets. The antimony adduct crystallizes in the orthorhombic *P*bca space group with one crystallographically unique molecule in the unit cell.

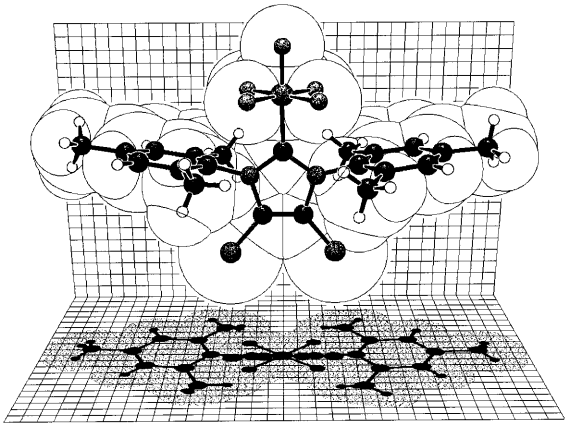

Fig. 3. KANVAS drawing of **2** · PF_5

The phosphorus in **2** · PF_5 shows a fairly regular octahedral environment in which the average of the four *cis*-angles to C^2 (89.2° [89.0°]) is smaller that the average of the other eight *cis*-angles (90.4° [90.5°]). The four equatorial fluorine atoms form a plane with a slight up-down alternating arrangement of the fluorines. The equatorial fluorine positions are only 0.3 [0.1] pm above or below this mean F_{eq}-plane. The phosphorus center is displaced by 2.4 [2.9] pm out of the F_{eq}-plane away from C^2. The plane of the equatorial fluorine atoms is inclined by 88.2° [83.2°] with respect to the plane of the imidazole ring. The imidazole ring is nearly planar, with no atom deviating more than 0.5 [0.6] pm from the mean plane. The phosphorus atom resides 5.8 [20.5] pm out of the imidazole mean plane and lies 1.5° [5.3°] off the idealized 2-fold imidazole axis. The nitrogen centers are essentially planar with N^1 and N^3 rising 5.0 [2.5] pm and 2.7 [1.9] pm above the planes of the three attached atoms. The N–C–N angle at the former carbene center of **2** · PF_5 is 106.9(3)° [105.1(3)°] which is similar to the angle observed in **1** · $PhPF_4$. The carbene-phosphorus bond distance in **2** · PF_5 is 189.8(3) [189.8(3)] pm and thus very similar to the corresponding value in **1** · $PhPF_4$ (191.0(4) [(191.0(4)] pm [13]. The P–C bond distance is, however, substantially longer than that observed for carbene-phosphinidene adducts (typically 117.1 ppm) [15, 16].

Similar to the situation for **2** · PF_5, **2** · AsF_5 shows a regular octahedral environment at arsenic in which the average of the four *cis*-angles to C^2 (89.8° [89.7°]) is only slightly smaller that the average of the other eight *cis*-angles (90.1° [90.2°]). The four equatorial fluorine atoms again form a plane with a slight up-down alternating arrangement of the fluorines. The equatorial fluorine positions are 0.9 [0.9] pm above or below the mean F_{eq}-plane. The arsenic center is only slightly displaced (0.7 [0.9] pm) out of the F_{eq}-plane away from C^2. The imidazole mean plane is nearly perpendicular (88.0° [82.6°]) to the plane of the equatorial fluorines. The imidazole ring is planar with no atom deviating more than 0.1 [0.5] pm from the average plane. The arsenic atom lies 7.0 [23.0] pm out of the plane of the average imidazole ring and deviates 2.2° [5.8°] from the idealized imidazole 2-fold axis. The nitrogen centers are also essentially planar with N^1 and N^3 rising 6.0

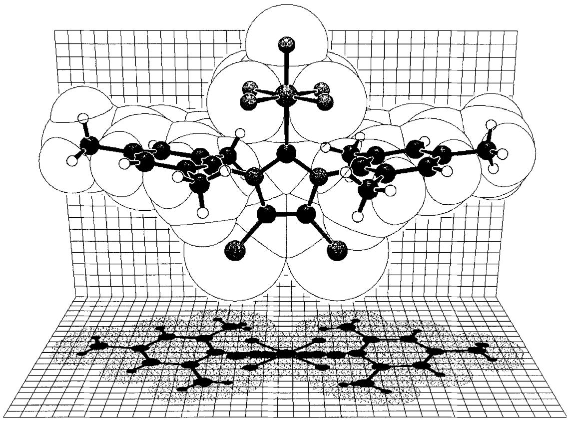

Fig. 4. KANVAS drawing of $\mathbf{2} \cdot AsF_5$

[2.6] pm and 2.4 [1.6] pm, respectively, above the planes of their three attached atoms. The N–C–N angle at the former carbene center of $\mathbf{2} \cdot AsF_5$ is 106.0(4)° [106.7(4)°]. Because of the larger pnictogen atom, the carbene-arsenic bond distance in $\mathbf{2} \cdot AsF_5$ (199.1(6) [200.6(5)] pm) is approximately 10 pm longer than the corresponding distance in $\mathbf{2} \cdot PF_5$ (189.8(3) [189.8(3)] pm). This C-As distance is again longer than observed for carbene-arsenic distances in arsenidine adducts (~190.0 pm) [15].

The antimony adduct $\mathbf{2} \cdot SbF_5$ exhibits an octahedral geometry at antimony that is less regular than the geometry at arsenic and is distorted in the opposite direction. The four equatorial fluorine atoms reside perfectly in a plane. The antimony center rises 1.5 pm out of the F_{eq}-plane, but is displaced towards C^2. The F_{eq}-plane is twisted 88.3° with respect to the imidazole plane. The imidazole ring is planar with no atom deviating more than 0.2 pm from the average plane. The antimony atom is 4.9 pm out of the plane of the average imidazole ring and lies 1.2° away from the idealized imidazole C_2 vector. The nitrogen centers are again essentially planar with N^1 and N^3 rising 3.8 pm and 0.8 pm above the planes of the three attached atoms. The N–C–N angle (105.2(4)°) at the former carbene center of

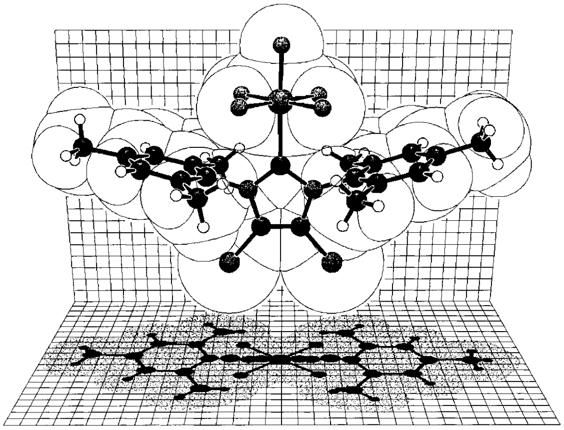

Fig. 5. KANVAS drawing of $\mathbf{2} \cdot SbF_5$

2 · SbF_5 is very similar to the corresponding angles in the lighter homologues. The carbene-antimony bond distance (217.5(5) pm) is ~15 pm longer than the arsenic-carbon distance in **2** · AsF_5. There is only one other imidazol-2-ylidene adduct involving an antimony; it is derived from carbene **2** and $Sb(CF_3)_3$ [8]. The C^2–Sb distance in **2** · $Sb(CF_3)_3$ is 282.1 pm and thus substantially longer that the carbene-antimony distance in **2** · SbF_5. However, the average antimony–carbon distance for the CF_3 groups in **2** · $Sb(CF_3)_3$ is 2.22 pm; these bonds more closely resemble the C–Sb distance in **2** · SbF_5.

All PnF_5 and BF_3 adducts of carbenes **1** and **2** described above have strong C^2-heteroatom bonds allowing no easy dissociation to the components electrophile and carbene. The strong nature of the bonds to the carbene centers is evidenced by the large upfield shifts of the ^{13}C resonances of the C^2 center in the adducts. These ^{13}C chemical shifts ($\delta \sim 160$ ppm) are all strongly upfield of the resonances for the carbene centers ($\delta \sim 220$ ppm) and approach shifts typical of an imidazolium cation ($\delta \sim 135$ ppm). The C^2 chemical shifts in the adducts reported herein are also similar to the adduct **3** ($\delta_{C^2} = 152$ ppm) which also contains a pnictogen (phosphorus) at C^2 with no *pπ-pπ* interactions to the imidazole ring [17].

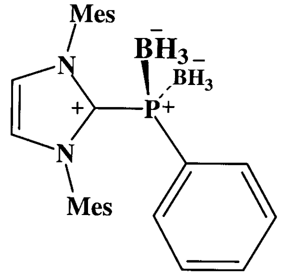

Mes = 1-(2,4,6-trimethylphenyl)

3

It was of interest to investigate the behavior of the boron trifluoride adduct **2** · BF_3 towards mercury(II) fluoride with a view to possible carbene-boron bond cleavage resulting in *bis*(carbene)-mercury tetrafluoroborates (Eq. 5). Similar carbene-mercury(II) salts have been reported from the mercuration of imidazolium salts [18, 19]. However, carbene-mercury complexes were not formed by heating a mixture of **2** · BF_3 with mercury(II) fluoride in acetonitrile. Proton and ^{19}F NMR spectra of the reaction mixture showed no evidence for the formation of the desired complex **4**. This is further indication that the carbon-boron bond in adducts like **2** · BF_3 is strong and not easily cleaved.

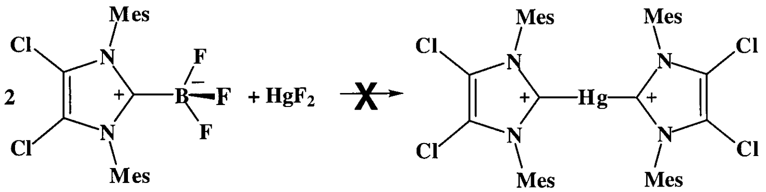

Mes = 1-(2,4,6-mesityl)

$2\,BF_4^-$

4

(5)

Conclusions

Nucleophilic carbenes can form stable adducts with strong electron acceptors such as pnictogen pentafluorides if the reactivity is moderated and a reaction medium is carefully selected. The imidazol-2-ylidene **1** that bears protons on the imidazole ring reacted with PF_5 to form the adduct $\mathbf{1} \cdot PF_5$. However, the major material isolated was identified as the simple imidazolium hexafluorophosphate $\mathbf{1} \cdot HPF_6$. In contrast, when the chlorinated carbene **2** was allowed to react with PF_5, the adduct $\mathbf{2} \cdot PF_5$ was isolated in a much higher yield. No C^2-protonated compounds were detected by ^{1}H NMR spectroscopy during the formation of $\mathbf{2} \cdot PF_5$. The improvement in adduct formation through the use of **2** is likely the result of a moderation of the carbene's nucleophilic reactivity by the inductive effect of the two chlorine substituents. Additionally, the acidic protons on $C^{4,5}$ of the product imidazolium ions are absent so that they cannot be abstracted by bases in the reaction medium.

The reaction between the nucleophilic carbene **2** and pnictogen pentafluorides could be extended to arsenic and antimony. In both cases, the reactions were carried out in 1,3-*bis*(trifluoromethyl)benzene as a reaction medium. The adducts $\mathbf{2} \cdot AsF_5$ and $\mathbf{2} \cdot SbF_5$ were stable solids that could be easily handled after their formation. The availability of NMR data and X-ray crystal structures for the family of PnF_5 adducts allows a comparison of these three compounds. Because of the larger size of the heavier pnictogen atoms, the carbene-pnictogen bond distances increase (189.8 (P), 199.9 (As), 217.5 (Sb) pm) along the sequence of structures. The octahedral geometries at the pnictogen centers are only slightly distorted. For $\mathbf{2} \cdot PF_5$, the phosphorus center is slightly displaced (~2.7 pm) out of the average plane of the equatorial fluorine atoms away from C^2. In the solid state structure of $\mathbf{2} \cdot SbF_5$, the antimony center is displaced towards C^2 by 1.5 pm from the plane of the equatorial fluorine atoms. The arsenic analogue adopts an intermediate geometry with only a very slight distortion (~0.8 pm) in the same direction as observed for $\mathbf{2} \cdot PF_5$. In the ^{19}F NMR spectra, the fluorine resonances of $\mathbf{2} \cdot SbF_5$ are observed at lower field compared to the corresponding values for $\mathbf{2} \cdot PF_5$ and $\mathbf{2} \cdot AsF_5$. This variation in chemical shifts is likely due to the stronger shielding exerted by antimony.

The pairs of carbene-derived adducts $\mathbf{1} \cdot BF_3$ and $\mathbf{2} \cdot BF_3$ as well as $\mathbf{1} \cdot PF_5$ and $\mathbf{2} \cdot PF_5$ show remarkable spectroscopic similarities regardless of the identify of the starting carbene. The close similarities in the ^{11}B or ^{31}P chemical shifts for analogous compounds suggest that bonding to the Lewis acid heteroatom (B or P) may be quite similar in spite of the large difference in stability and reactivity between the carbenes **1** and **2**. In the case of the BF_3 adducts, for which solid state structures of both $\mathbf{1} \cdot BF_3$ and $\mathbf{2} \cdot BF_3$ are available, the C^2–B bond distances do show a dependence on the identify of the carbene fragment. The C–B distance in $\mathbf{2} \cdot BF_3$ (166.9 pm) is longer than in $\mathbf{1} \cdot BF_3$ (163.5 pm), indicating a weaker carbene-boron bond in $\mathbf{2} \cdot BF_3$ as might be expected for the less nucleophilic carbene **2**. The difference in the C^2–B bond distances between $\mathbf{1} \cdot BF_3$ and $\mathbf{2} \cdot BF_3$ and the similarity in the ^{11}B shifts may be an indication that ^{11}B (or ^{31}P) NMR spectra are not sensitive indicators of electronic variations among these carbene adducts.

The high stability and solvent insensitivity of the $\mathbf{2} \cdot PnF_5$ adducts after their formation, along with the failure to observe carbene transfer to a mercury center (in the case of **2** · BF_3), indicate that these *Lewis* acid adducts do not undergo facile dissociation of the carbene fragment as has been observed for adducts with weaker *Lewis* acids.

Experimental

All experiments and manipulations were carried out under an atmosphere of dry nitrogen, either in a dry box or using standard Schlenk techniques. Solvents were dried using standard procedures and distilled in a nitrogen atmosphere prior to use unless otherwise indicated. Deuterated solvents were dried over molecular sieves (3 Å or 4 Å). Glassware was oven-dried at 160°C overnight. For condensations of gases, liquid nitrogen was used for cooling and gas (PF_5, AsF_5) transfers were carried out on a Kel-F greased high vacuum line. Gases at a known pressure in a manifold of defined volume (235 cm^3) were condensed into the reaction vessel until the pressure drop in the main manifold corresponded to the desired amount of the reagent.

NMR spectra (^{1}H, ^{11}B, ^{13}C, ^{19}F, and ^{31}P) were recorded in the NMR laboratory of the Chemical Institutes of *Technische Universität Braunschweig* and at the *Institut für Anorganische und Analytische Chemie der Technischen Universität Braunschweig* (Bruker AC 200; ^{1}H at 200.1 MHz, ^{13}C at 50.3 MHz, ^{19}F at 188.3 MHz, ^{31}P at 81.0 MHz) or at the DuPont Corporate Center for Analytical Science of the DuPont Experimental Station in Wilmington, Delaware, USA. on the following spectrometers: General Electric QE-300 (^{1}H at 300.5 MHz, ^{13}C at 75.6 MHz, ^{31}P at 121.7 MHz), General Electric Omega 300WB (^{1}H at 300.5 MHz, ^{11}B at 96.4 MHz, ^{13}C at 75.6 MHz, ^{19}F at 282.7 MHz, ^{31}P at 121.7 MHz), Bruker DPX 300 (^{1}H at 300.1 MHz, ^{13}C at 75.5 MHz, ^{19}F at 282.4 MHz, ^{31}P at 122.3 MHz), Varian Unity Nova 400 (^{1}H at 400.0 MHz, ^{13}C at 100.6 MHz), and Bruker DRX 400 (^{19}F at 376.9 MHz). The chemical shifts are referenced as followed: ^{1}H, ^{13}C: $(CH_3)_4Si$; ^{11}B; $BF_3 \cdot Et_2O$; ^{19}F: $CFCl_3$; ^{31}P: ext. 85% H_3PO_4.

1,3-Dimesitylimidazolium-2-trifluoroborate (**1** · BF_3)

Boron trifluoride etherate (186 mg, 1.31 mmol) was added to a solution of 400 mg (1.31 mmol) of **1** in 20 cm^3 of *THF* at 0°C. The reaction mixture was allowed to warm to room temperature and stirred for 30 min. A colorless precipitate formed which was collected by filtration and dried *in vacuo*. **1** · BF_3 was recrystallized from hot acetonitrile.

Yield: 402 mg (82%); m.p.: 375–377°C (dec); ^{1}H NMR (300.1 MHz, CD_3CN): $\delta = 2.05$ (s, 12H, *ortho*-CH_3), 2.35 (s, 6H, *para*-CH_3), 7.05 (s, 4H, *meta*-CH), 7.28 (s, 2H, NCH) ppm; ^{11}B NMR (96.4 MHz, CD_3CN, 70°C): $\delta = -1.36$ (q, $^1J_{BF} = 34.6$ Hz ppm; ^{13}C $\{^1$H$\}$ NMR (100.6 MHz, CD_3CN, 70°C): $\delta = 17.59$ (s, *ortho*-CH_3), 21.33 (s, *para*-CH_3), 124.60 (s, NCH), 129.95 (s, C_{meta}), 135.52 (s, C^{ipso}), 136.25 (s, C^{ortho}), 140.85 (s, C^{para}), 160.2 (m, C^2) ppm; ^{13}C $\{^{19}$F$\}$ NMR (100.6 MHz, CD_3NO_2, 90°C): $\delta = 161.3$ (q, $^1J_{BC} = 82$ Hz, C^2) ppm; ^{19}F NMR (282.4 MHz, CD_3CN): $\delta = -142.44$ (q, $^1J_{FB} = 34.6$ Hz) ppm; $C_{21}H_{24}N_2BF_3$ (372.24); calcd.: C 67.76, H 6.50, N 7.53; found: C 67.53, H 6.61, N 7.75.

1,3-Dimesitylimidazolium-2-pentafluorophosphate (**1** · PF_5)

In a dry box, a heavy-walled glass tube was charged with 100 mg (0.33 mmol) of **1** and 5 cm^3 of toluene. The tube was then connected to a high vacuum transfer line and onto this frozen solution, 41 mg (0.33 mmol) of phosphorus pentafluoride were condensed at −196°C. The mixture was warmed to −80°C, stirred for 1.5 h, and subsequently warmed to 60°C. After stirring for 21.5 h an orange solid and a red solution formed. The mixture was filtered to give 107 mg of a yellow solid that contained 1,3-dimesitylimidazolium hexafluorophosphate (**1** · HPF_6) as the major product. The solvent from the red filtrate was removed *in vacuo* to give 32 mg of a red solid containing **1** · PF_5 and trace amounts of $\mathbf{1}\cdot\mathrm{HPF}_6$. The adduct $\mathbf{1}\cdot\mathrm{PF}_5$ proved to be difficult to handle. During recrystallization from *THF*, $\mathbf{1}\cdot\mathrm{PF}_5$ was converted to additional $\mathbf{1}\cdot\mathrm{HPF}_6$ and other (unidentified) byproducts. The following data apply to the crude products.

$1\cdot\mathrm{PF}_5$: ^{1}H NMR (200.1 MHz, *THF* d_8): $\delta = 2.07$ (s, 12H, *ortho*-CH_3), 2.33 (s, 6H, *para*-CH_3), 6.98 (s, 4H, *meta*-CH) , 7.42 (d, 2H, $^4J_{\mathrm{HP}} = 2.4$ Hz, NCH) ppm; ^{1}H NMR (200.1 MHz, toluene-d_8): $\delta = 2.05$ (s, 12H, *ortho*-CH_3), 2.33 (s, 6H, *para*-CH_3), 6.88 (s, 4H, *meta*-CH), 7.12 (s, 2H, NCH) ppm; ^{13}C {^{1}H} NMR (50.3 MHz, *THF*-d_8): $\delta = 17.96$ (m, *ortho*-CH_3), 21.41 (s, *para*-CH_3), 124.68 (d, $^3J_{\mathrm{CP}} = 8.6$ Hz, NCH), 129.68 (s, C^{meta}) 136.13 (s, C^{ortho}), 136.67 (s, C^{ipso}), 140.20 (s, C^{para}) ppm; C^2 not observed; ^{19}F NMR (188.3 MHz, toluene-d_8): $\delta = -77.34$ (dquint, 1F, $^1J_{\mathrm{FP}} = 772.0$ Hz, $^2J_{\mathrm{FF}} = 54.4$ Hz, PF_4F), -53.57 (dd, 4F, $^1J_{\mathrm{FB}} = 784.8$ Hz, $^2J_{\mathrm{FF}} = 54.4$ Hz, $\mathrm{P}F_4\mathrm{F}$) ppm; ^{31}P{^{1}H} NMR (81.0 MHz, *THF*-d_8): $\delta = -148.40$ (dquint, $^1J_{\mathrm{PF}} = 763.9$ Hz, $^1J_{\mathrm{PF}} = 786.3$ Hz, $\mathrm{PF}_4\mathrm{F}$) ppm; ^{31}P{^{1}H} NMR (81.0 MHz, toluene-d_8): $\delta = -151.28$ (dquint, $^1J_{\mathrm{PF}} = 785.2$ Hz, $^1J_{\mathrm{PF}} = 771.4$ Hz, $\mathrm{PF}_4\mathrm{F}$) ppm.

$\mathbf{1}\cdot\mathrm{HPF}_6$: ^{1}H NMR (200.1 MHz, *THF*-d_8): $\delta = 2.17$ (s, 12H, *ortho*-CH_3), 2.36 (s, 6H, *para*-CH_3), 7.14 (s, 4H, *meta*-CH), 7.96 (s, 2H, NCH), 9.16 (s, 1H, C^2H) ppm; ^{19}F NMR (188.3 MHz, toluene-d_8): $\delta = -70.83$ (d (br), $^1J_{\mathrm{FP}} = 710.0$ Hz, PF_6) ppm; ^{31}P{^{1}H} NMR (81.0 MHz, *THF*-d_8): $\delta = -140.38$ (sept, $^1J_{\mathrm{PF}} = 710.0$ Hz, PF_6) ppm.

1,3-Dimesityl-4-5-dichloromidazolium-2-trifluoroborate ($\mathbf{2}\cdot\mathrm{BF}_3$)

Boron trifluoride etherate (190 mg, 1.34 mmol) was added to a solution of 500 mg (1.34 mmol) of **2** in 20 cm^3 of *THF* at 0°C. The reaction mixture was allowed to warm to room temperature and stirred for 1 h. Removing of the volatiles *in vacuo* gave $\mathbf{2}\cdot\mathrm{BF}_3$ as a colorless solid that was recrystallized from hot tuluene to afford 491 mg (83%) of the crystalline adduct.

M.p.: 248°C (dec); ^{1}H NMR (300.1 MHz, $\mathrm{C}_6\mathrm{D}_6$): $\delta = 2.01$ (s, 6H, *para*-CH_3), 2.03 (s, 12H, *ortho*-CH_3), 6.68 (s, 4H, *meta*-CH) ppm; ^{11}B NMR (96.4 MHz, $\mathrm{CD}_3\mathrm{CN}$): $\delta = -1.65$ (q, $^1J_{\mathrm{BF}} = 30.5$ Hz) ppm; ^{13}C {^{1}H} NMR (75.6 MHz, $\mathrm{C}_6\mathrm{D}_6$): $\delta = 17.31$ (s, *ortho*-CH_3), 21.01 (s, *para*-CH_3), 118.3 (s, NCCl), 129.59 (s, C^{meta}), 131.06 (s, C^{ipso}), 135.32 (s, C^{ortho}), 140.57 (s, C^{para}), 162.82 (qq, $^1J_{\mathrm{CB}} = 78$ Hz, $^2J_{\mathrm{CF}} = 66$ Hz, C^2) ppm; ^{19}F NMR (376.9, $\mathrm{CD}_3\mathrm{CN}$): $\delta = -142.62$ (q, $^1J_{\mathrm{FB}} = 32.4$ Hz) ppm; $\mathrm{C}_{21}\mathrm{H}_{22}\mathrm{N}_2\mathrm{BCl}_2\mathrm{F}_3$ (441.13); calcd.: C 57.18, H 5.03, N 6.35; found: C 57.43, H 5.01, N 6.27.

1,3-Dimesityl-4,5-dichloroimidazolium-2-pentafluorophate ($\mathbf{2}\cdot\mathrm{PF}_5$)

Phosphorus pentafluoride (119 mg, 0.94 mmol) was condensed onto a frozen solution of 350 mg (0.94 mmol) of 4,5-dichloro-1,3-dimesitylimidazol-2-ylidene (**2**) in 10 cm^3 of toluene at −198°C. After warming to room temperature a colorless solid formed that was collected by filtration and dried *in vacuo*. Crystals of $\mathbf{2}\cdot\mathrm{PF}_5$ were obtained from a *THF*/toluene (3:1) solution at −20°C.

Yield: 271 mg (57.8%): m.p.: 268°C (dec); ^{1}H NMR (300.5 MHz, *THF*-d_8): $\delta = 2.07$ (s, 12H, *ortho*-CH_3), 2.35 (s, 6H, *para*-CH_3), 7.06 (s, 4 H, *meta*-CH) ppm; ^{13}C{^{1}H ^{19}F} NMR (100.6 MHz, *THF*-d_8): $\delta = 17.68$ (s, *ortho*-CH_3), 21.20 (s, *para*-CH_3), 120.42 (d, $^3J_{\mathrm{CP}} = 9.8$ Hz, NCCl), 129.84 (s, C^{meta}), 132.73 (s, C^{para}), 136.49(s, C^{ortho}), 141.36 (s, C^{ipso}), 161.41 (d, $^1J_{\mathrm{CP}} = 290.6$ Hz, C^2) ppm; ^{19}F NMR (376.9 MHz, *THF*-d_8): $\delta = -83.61$ (dquint 1F, $^1J_{\mathrm{PF}} = 772.8$ Hz, $^2J_{\mathrm{FF}} = 55.2$ Hz, F_{ax}), -58.01 (dd, 4F, $^1J_{\mathrm{PF}} = 788.6$ Hz, $^2J_{\mathrm{FF}} = 55.2$ Hz, F_{eq}) ppm; ^{31}P{^{1}H} NMR (121.7 MHz, *THF*-d_8): $\delta = -151.79$ (dquint $^1J_{\mathrm{PF}} = 772.3$ Hz, $^1J_{\mathrm{PF}} = 785.8$ Hz) ppm; $\mathrm{C}_{21}\mathrm{H}_{22}\mathrm{N}_2\mathrm{Cl}_2\mathrm{F}_5\mathrm{P}$ (449.29); calcd.: C 50.52, H 4.44, N 5.61, Cl 14.2, F 19.0, P 6.20; found : C 50.68, H 4.46, N 5.61, Cl 140.0, F 18.8, P 6.24.

1,3-Dimesityl-4,5-dichloroimidazolium-2-pentafluoroarsenate ($\mathbf{2}\cdot\mathrm{AsF}_5$)

Arsenic pentafluoride (160 mg, 0.94 mmol) was condensed onto a frozen solution of 350 mg (0.94 mmol) of **2** in 10 cm^3 of 1,3-*bis*(trifluoromethyl)benzene at −198°C. After warming to room temperature, a clear orange solution was formed which was stirred for 1 h and then stored at −25°C for 1 d. The solvent volume was reduced by 75% to precipitate a pale orange solid that was collected by filtration. The filter cake was dried by a stream of nitrogen gas. Crystals of **2** · AsF_5 were obtained form a *THF* solution at −20°C.

Yield: 330 mg (64.6%); m.p.: 305–307°C (dec); ^{1}H NMR (300.1 MHz, *THF*-D_8): $\delta = 2.09$ (S, 12H, *ortho*-CH_3), 2.36 (s, 6H, *para*-CH_3), 7.07 (s, 4H, *meta*-CH) ppm $^{13}C\{^1H\}$ NMR (75.5 MHz, *THF*-d_8): $\delta = 17.70$ (s, *ortho*-CH_3), 21.21 (s, *para*-CH_3), 121.98 (s, NCCl), 129.91 (s, C^{meta}), 132.09 (s, C^{para}), 136.71 (s, C^{ortho}}, 141.92 (s, C^{ipso}) ppm; $^{13}C\ \{^{19}F\}$ NMR (100.6 MHz, *THF*-d_8): $\delta = 17.76$ (q, $^1J_{CH} = 127.7$ Hz, *ortho*-CH_3), 21.23 (q, $^1J_{CH} = 126.7$ Hz, *para*-CH_3), 122.06 (s, NCCl), 129.93 (d, $^1J_{CH} = 158.7$ Hz, C^{meta}), 132.09 (S, C^{para}), 136.76 (s, C^{ortho}), 141.95 (s, C^{ipso}), 158.31 (s, C^2) ppm; ^{19}F NMR (282.4 MHz, *THF*-d_8): $\delta = -68.06$ (quint, 1F, $^2J_{FF} = 114.6$ Hz, F_{ax}], −45.97 (d, 4F, $^2J_{FF} = 111.1$ Hz, F_{eq} ppm.

Table 2. X-Ray structural data for carbene-BF_3 and carbene-*Pn*F_5 adducts

	1 · BF_3	**2** · BF_3	**2** · PF_5	**2** · AsF_5	**2** · SbF_5
Formula	$C_{21}H_{24}N_2BF_3$	$C_{21}H_{22}N_2BCl_2F_3$	$C_{21}H_{22}N_2Cl_2PF_5$	$C_{21}H_{22}N_2AsCl_2F_5$	$C_{21}H_{22}N_2Cl_2F_5Sb$
Growth method	acetonitrile, 23°C	toluene, 60°C	*THF*/toluene, −20°C	*THF* −20°C	*THF*−20°C
Color	colorless	colorless	colorless	colorless	colorless
Symmetry	monoclinic	monoclinic	monoclinic	monoclinic	orthorombic
Space group	*P*2_1/c (No. 14)	*I*2/a (No. 15)	*C*c (No.9)	*C*c (No. 9)	*P*bca (No. 61)
a Å	8.366(2)	17.064(5)	8.762(1)	8.862(1)	17.362(1)
b Å	14.657(1)	14.508(3)	29.409(1)	29.445(2)	17.248(1)
c Å	16.542(4)	17.655(2)	17.310(1)	17.384(1)	15.936(1)
β (deg)	103.89(1)	91.612(2)	92.89(1)	92.95(1)	(90)
temperature (°C)	−55	−80	−100	−100	−100
μ (Mo) (cm^{-1})	0.88	3.30	4.13	17.84	14.37
Diffractometer	Enraf-Nonius CAD4	Enraf-Nonius CAD4	Rigaku RU300	Rigaku RU300	Rigaku RU300
Scan method	ω	ω	area detection	area detection	area detection
Data octants	+++, −++	+++, −++	all	all	all
2θ	≥2.5°,≤55.0°	≥3.3°, ≤50.0°	≥6.2°, ≤48.2°	≥3.6°, ≤48.2°	≥4.2°, ≤48.2°
Maximum *hkl*	10 19 21	20 17 20	10 33 19	9 33 19	19 19 18
Data collected	4836	3675	12332	12260	20958
Duplicates	–	–	4467	4343	3457
R_{int}>-Merge (%)	–	–	1.6	2.0	3.1
No. of unique data (I ≤3.0σ(I))	1518	1809	3311	3165	2374
Solution method	direct methods (SHELXS)	direct methods (MULTAN)	direct methods (MULTAN)	direct methods (MULTAN)	direct methods (SHELXS)
Anomalous disp.	none	Cl	P, Cl	As, Cl	Sb, Cl
Parameters varied	271	262	557	557	280
Data/para.ratio	5.60	6.90	5.93	5.67	8.46
R, R_w	0.066, 0.048	0.048, 0.041	0.030, 0.038	0.030, 0.031	0.038, 0.037
Error of fit	1.44	1.31	2.33	1.58	1.60
Max shift Δ/σ	0.10	0.00	0.01	0.01	0.00
Max residual density (e/$Å^3$)	0.25	0.33	0.17	0.29	0.50
Cambridge ref. no.	132900	132901	132902	132903	132904

1,3-Dimesityl-4,5-dichloroimidazolium-2-pentafluoroantimonate (**2** · SbF$_5$)

A solution of 185 mg (0.50 mmol) of **2** in 5 cm^3 of 1,3-*bis*(trifluoromethyl)benzene was added to 107 mg (0.50 mmol) of antimony pentafluoride at 0°C. The color changed from yellow to red. After 1 m stirring at room temperature, 5 cm^3 of perfluoro-*n*-hexane were added, and **2** · SbF$_5$ was precipitated as a slightly pink solid. The solid was collected by filtration and washed with perfluoro-*n*-hexane. Crystalline **2** · SbF$_5$ was obtained by recrystallization of the crude product from a *THF* solution at −20°C.

Yield: 225 mg (77.1%); m.p.: 265–267°C(dec); ^{1}H NMR (300.1 MHz, C$_6$D$_6$): $\delta = 1.98$ (s, 12H, *ortho*-CH$_3$), 2.00 (s, 6H, *para*-CH$_3$), 6.89 (s, 4 H, *meta*-CH) ppm; ^{1}H NMR (300.1 MHz, *THF*-d$_8$): $\delta = 2.11$ (s, 12H, *ortho*-CH$_3$), 2.37 (s, 6H, *para*-CH$_3$), 7.09 (s, 4H, *meta*-CH) ppm; ^{13}C{^{1}H} NMR (75.5 MHz, *THF*-d$_8$): $\delta = 17.45$ (s, *ortho*-CH$_3$), 21.03 (s, *para*-CH$_3$), 122.24 (s, NCCl), 129.64 (s, C^{meta}), 130.32 (s, C^{para}), 136.05 (s, C^{ortho}), 141.77 (s, C^{ipso}) ppm C2 not observed; ^{19}F NMR (282.4 MHz, C$_6$D$_6$); $\delta = -122.28$ (m (br), 1F, F_{ax}), −99.47 (m (br), 4F, F_{eq}) ppm.

X-Ray structural analyses

The X-ray data are presented in Table 2. No absorption corrections were applied. Model refinement was accomplished by full-matrix least squares fit on F. All non-hydrogen atoms were refined with anisotropic thermal parameters, and hydrogens were placed in fixed positions. All data were collected using MOK_α radiation and a graphite monochromator.

Acknowledgements

AJA and *RS* thank the DuPont Company for their support of parts of this work (Contribution Nr. 7730). *RK* gratefully acknowledges the support of DuPont and the *Universität Braunschweig* that enabled a visit to the DuPont Experimental Station. *AJA* is grateful to the *Alexander von Humboldt Stiftung* for a senior research prize that facilitated this work.

References

[1] Arduengo AJ III (1999) Acc Chem Res **32**: 913
[2] Arduengo AJ III, Krafczyk R (1998) Chemie in unserer Zeit **32:** 6
[3] Herrmann WA, Köcher C (1997) Angew Chem **109**: 2256
[4] Arduengo AJ III, Tamm M, Calabrese JC, Davidson F, Marshall WJ (1999) Chem Lett 1021
[5] Alder RW, Blake ME, Bortolotti C, Bufali S, Butts CP, Linehan E, Oliva JM, Orpen AG, Quayle MJ (1999) Chem Commun (Cambridge) 241
[6] Wacker A, Pritzkow H, Siebert W (1998) Eur J Inorg Chem 843
[7] Arduengo AJ III, Kline M, Calabrese JC, Davidson F (1991) J Am Chem Soc **113**: 9704
[8] Arduengo AJ III, Krafczyk R, Mahler W, Marshall WJ, Schmutzler R (1999) Z Anorg Allg Chem **625**: 1813
[9] Arduengo AJ III, Goerlich JR, Davidson F, Marshall WJ (1999) Z Naturforsch **54B**: 1350
[10] Kuhn N, Henkel G, Kratz T, Kreutzberg J, Boese R, Maulitz AH (1993) Chem Ber **126**: 2041
[11] Arduengo AJ III, Dias HVR, Harlow RL, Kline M (1992) J Am Chem Soc **114**: 5530
[12] Arduengo AJ III, Davidson F, Dias HVR, Goerlich JR, Khasnis D, Marshall WJ, Prakasha TK (1997) J Am Chem Soc **119**: 12742
[13] Arduengo AJ III, Krafczyk R, Marshall WJ, Schmutzler R (1997) J Am Chem Soc **119**: 3381

[14] Krafczyk R (1998) PhD Thesis, Technische Universität Braunschweig, Germany

[15] Arduengo AJ III, Calabrese JC, Cowley AH, Dias HVR, Goerlich JR, Marshall WJ, Riegel B (1997) Inorg Chem **36**: 2151

[16] Arduengo AJ III, Dias HVR, Calabrese JC (1997) Chem Lett **1997**: 143

[17] Arduengo AJ III, Carmalt CJ, Clyburne JAC, Cowley AH, Pyati R (1997) Chem Commun 981

[18] Wanzlick H-W, Schönherr H-J (1968) Angew Chem Int Ed Engl **7**: 141

[19] Arduengo AJ III, Marshall WJ Harlow RL, Prakasha TK (1996) Heteroatom Chem **7**: 421

Received September 6, 1999. Accepted (revised) October 20, 1999